

Resonance spins and the t dependence of Regge residues in multiperipheral models*

J. W. Dash[†]

Argonne National Laboratory, Argonne, Illinois 60439

S. T. Jones[‡]

Department of Physics and Astronomy, University of Alabama, University, Alabama 35486

(Received 12 June 1974)

We argue that the t dependence of Regge residues for small t can be understood within the context of multiperipheral cluster models if the clusters are identified with the resonance spectrum and the correct spin structure is included for the resonances. The difference between the slopes of the pp and πp differential cross sections is ascribed to the average shift of resonance spin by $1/2$ between the baryon and meson resonances. An illustrative calculation is performed which leads to qualitative agreement with experiment, including the energy dependence of diffractive slopes, multiplicities, and transverse momentum distributions for energies below 30 GeV. Longitudinal components of momentum transfer are correctly treated.

I. INTRODUCTION

The determination of the t dependence of Regge residues has been one of the outstanding problems in hadron physics. Two-body data indicate that differential cross sections $d\sigma/dt$ behave at fixed s and small t roughly like Ae^{Ct} , where C is typically a large number. At $s = 60 \text{ GeV}^2$, $C = 8 \text{ GeV}^{-2}$ for πp elastic scattering, while $C = 10 \text{ GeV}^{-2}$ for pp elastic scattering. Now since multiperipheral models generate Regge poles and since Regge poles are widely believed to have some relevance to the discussion of two-body data near $t=0$, it is tempting to imagine that some specific multiperipheral model might exist which could describe the t -dependence of Regge residues.¹ Attempts along this line have encountered difficulties at several points. The first is the requirement of generating a sensible trajectory function.² Not every ladder model will do this. This is related to the energy dependence of the slope parameters and to associated momentum transfer and transverse momentum distributions of produced particles, as we shall discuss. The second point concerns the reasonably straightforward (and related) problem of generating a reasonable multiplicity of produced particles by the multiperipheral chain.³ It is known that if the multiperipheral model is multiperipheral in clusters with exchanged masses small compared to the masses of the clusters, these two problems can be overcome. However, the nature of the clusters is crucial. Some discussions assume that the clusters have no spin and decay isotropically in their own rest frame. However, we will see that this assumption leads to the prediction that the slopes of the πp and pp cross sections should be equal, and in any case these slopes will turn out

much too small.⁴

Our assumption is different. Following several authors^{5,6} we shall assume that *the spins of the clusters are directly related to the nature of the Regge residues*. In particular we suggest that the clusters forming the multiperipheral components are predominantly the first few meson and baryon resonances. To agree with the data, all baryons must be confined to the ends of the multiperipheral chain, as illustrated in Fig. 1(a) for πp scattering and Fig. 1(b) for pp scattering. Effects related to baryon exchange are secondary. Once this is assumed, the existence of elastic diffractive slopes, and the fact that there should be some difference between the πp and pp slopes, are qualitatively easy to understand. Since the multiperipheral chain sums to a Regge pole (call it \hat{P}), the $pp\hat{P}$ vertex is controlled by the first

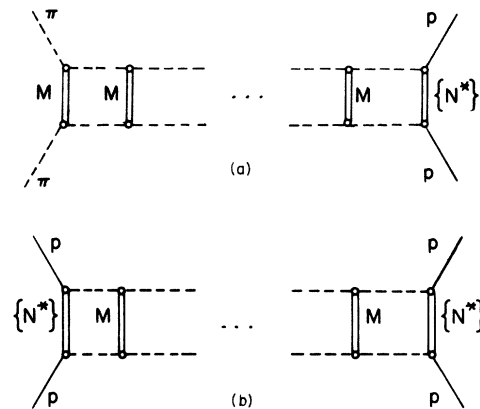


FIG. 1. (a) Model for the imaginary part of the πp scattering amplitude at intermediate energies. (b) Model for pp scattering at intermediate energies.

few baryon resonances $\{N, \Delta(1236), \dots\}$, whose average spin is called J_B . The model for the vertex is shown in Fig. 2. For simplicity we assume that the connecting propagators with momentum transfers t_1 and t_2 are pions, which are assumed to have spins close to zero. Such an assumption is not necessary and could be relaxed, but it is certainly reasonable if the average momentum transfers $\langle t_i \rangle$ are small, which will be true if t is small. Let us assume that the helicities of the protons in Fig. 1 are $+\frac{1}{2}$. The off-shell scattering process $\pi(t_1) + p \rightarrow N^* \rightarrow \pi(t_2) + p'$ inside the loop integral produces a rotation matrix function $d_{1/2, 1/2}^{J_B}(\theta_B)$, where θ_B is the off-shell scattering angle for this (virtual) process. At $t=0$, $\theta_B=0$. This d^{J_B} function provides a peripheral cutoff in θ_B which helps cut off the t_i integrations and ultimately results in a cutoff in t . This cutoff is in addition to any peripherality due to the propagators in t_1 and t_2 , and is primarily responsible for the peripheral nature of the baryon vertex function. Now the $\pi\pi\hat{P}$ vertex is controlled by the $\pi\pi$ resonance spectrum in our model, as illustrated in Fig. 3. We have again assumed π exchange. Denoting the average meson spin by J_M , the in-ternal $\pi(t_1) + \pi \rightarrow M \rightarrow \pi(t_2) + \pi'$ scattering amplitude with over-all scattering angle θ_M produces a rotation function $d_{00}^{J_M}(\theta_M)$. For $J_M > 0$, this function will enhance the peripherality of the $\pi\pi\hat{P}$ vertex function.

The crucial point is now simply that

$$J_B \approx J_M + \frac{1}{2}.$$

That is, the average spin of the baryon spectrum $\{N, \Delta(1236), \dots\}$ is displaced in spin by $\frac{1}{2}$ unit from the meson resonance spectrum $\{\sigma, \rho, \dots\}$. Since as J increases $d_{\mu\mu}^J(z)$ becomes more peripheral in z , we expect that the d^{J_B} rotation function will provide a faster cutoff in t than will d^{J_M} . This is the essence of our assumption. It now remains to be seen whether the mechanism we have proposed can reasonably be expected to provide the large slopes of the πp and $p p$ differential cross sections as well as the differences between them, consistent with their energy dependence.

To approach this question, we have assumed a simple, though reasonable model. We assume that the $\pi\pi$ resonance spectrum is dominated by the ρ , while the πp spectrum is controlled by the $\Delta(1236)$. A multiperipheral chain of ρ mesons with pion exchange and baryon resonances at the ends is an idealized model, but it nevertheless is actually not phenomenologically wrong in any gross sense at intermediate energies, say $5 \text{ GeV}/c < p_{\text{lab}} < 30 \text{ GeV}/c$.⁷⁻¹⁰ In this range, inelastic diffraction, $K\bar{K}$, and baryon-antibaryon ($B\bar{B}$) production cross sec-

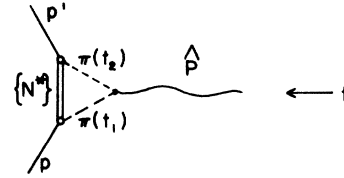


FIG. 2. Model for the $pp\hat{P}$ vertex.

tions are small, and the main corrections to the model come from other clustering effects involving other resonances ($\sigma, f; A_1, g$, etc.). We see no reason why a more complicated spectral assumption would invalidate our results which depend only on the general statement that $J_B \approx J_M + \frac{1}{2}$.

We close the Introduction with a few technical comments which are necessary to interpret our results. Those wishing to plunge into the calculation may proceed to Sec. II directly. Our simple illustrative model is a multiperipheral approximation σ_{sf}^M to what has become known as the single fireball cross section σ_{sf} .^{7,11,12} Caution should be exercised in utilizing the word fireball; we mean that the single fireball cross section has no diffraction nor $K\bar{K}$, $B\bar{B}$ production anywhere in subenergies in the production amplitude. Any such diffractive effect is termed "inelastic diffraction." It leads to a positive cross section $\sigma_{\text{inel}}^{\text{diff}}$ (Ref. 11) and negative absorptive corrections to σ_{sf} , called $\sigma_{\text{sf}}^{\text{abs}}$.^{12b} The $K\bar{K}$ and $B\bar{B}$ production cross section is called σ_B , and we write $\sigma_H = \sigma_{\text{inel}}^{\text{diff}} + \sigma_{\text{sf}}^{\text{abs}} + \sigma_B$. The total cross section $\sigma_{\text{tot}} \cong \sigma_{\text{sf}}^M + \sigma_{\text{el}} + \sigma_H$. The assumption made is that σ_H has an effective kinematic threshold at around $30 \text{ GeV}/c$, and that below this momentum $\sigma_{\text{tot}} \approx \sigma_{\text{sf}}^M + \sigma_{\text{el}}$. In the j plane we have two functions that have relevance. These we call $A_j(0)$, the partial-wave transform of σ_{tot} , and $\hat{A}_j(0)$, which is the partial-wave transform of σ_{sf}^M . The leading Regge pole we are talking about is an $I_t = 0$ pole at $j = \hat{\alpha}(0)$ in the function

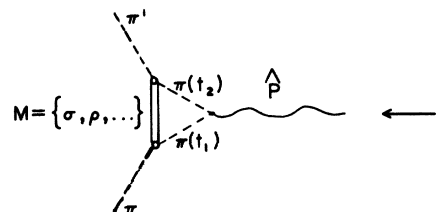


FIG. 3. Model for the $\pi\pi\hat{P}$ vertex.

$\hat{A}_j(0)$. It is termed the bare Pomeron, \hat{P} . The leading energy dependence of the cross section σ_{sf}^M has the simple form $\hat{\beta}(0)(s/s_0)^{\hat{\alpha}(0)-1}$ and it describes the leading behavior of σ_{tot} below the threshold of σ_H . Corrections involve $\hat{P} \times \hat{P}$ cuts¹⁰ which arise from simple "nonenhanced" absorptive corrections to σ_{sf}^M not included in σ_{sf}^{abs} . The alternative description of σ_{tot} below 30 GeV/c in terms of "renormalized" singularities of the usual amplitude A_j is extremely complicated. Above the intermediate-energy region, however, σ_H becomes important, and the energy dependence due to the "renormalized" singularities in A_j provides the appropriate description.¹¹ Enough phenomenology has been performed in the context of this approach to provide at least some motivation for regarding our idealized model as being phenomenologically sensible. This has involved exclusive⁸ and inclusive^{7,9} inelastic phenomenology as well as intermediate-energy two-body phenomenology utilizing the bare Pomeron.¹⁰ The residue functions we shall be concerned with in this work are therefore the residues of the bare Pomeron pole (\hat{P}) at $j = \hat{\alpha}(t)$ in the unrenormalized partial-wave amplitude $\hat{A}_j(t)$, which at $t=0$ is the partial-wave projection of $\sigma_{sf}^M(s)$. The continuation to $t \neq 0$ is made by regarding the model as a model for the \hat{P} component of the imaginary part of the elastic amplitude $T(s, t)$ below 30 GeV/c. Any discussion of cross sections at ISR energies would have to be supplemented by a discussion of inelastic diffraction and $K\bar{K}$, $B\bar{B}$ production processes. We shall not do this here, but it should be recognized that it is a consistent procedure first to examine the properties of the bare Pomeron \hat{P} and then to examine renormalization effects.

In the discussion which follows, it is important to recognize that the apparently "asymptotic" \hat{P} pole expression for the single fireball cross section $\sigma_{sf} \approx \hat{\beta}(0)s^{\hat{\alpha}(0)-1}$ is actually a good *finite*-energy approximation, even at energies only somewhat above that required for producing two resonances, which is $\ln s \gtrsim 2$.^{8,9} The basic finite-energy modification involves damped oscillations about the \hat{P} energy dependence (see Fig. 6 of Ref. 9). Our definition of intermediate energies (5–30 GeV/c) is consistent with the statement that the \hat{P} energy dependence is a reasonably accurate representation of σ_{sf} at intermediate s given the fact that the resonance clusters in σ_{sf} probably consist mostly of two or four pions. The latter statement is motivated by phenomenology⁸ and we shall calculate average multiplicities. The idea that $\sigma_{inel} \approx \sigma_{sf} \approx \hat{\beta}(0)s^{\hat{\alpha}(0)-1}$ is also consistent with all $0^{-\frac{1}{2}+} \rightarrow 0^{-\frac{1}{2}+}$ data at intermediate energies.¹⁰ We shall utilize the fit of Ref. 10 in order to extract secondary pole (e.g., ρ, A_2, \dots) and cut terms from

the elastic amplitudes. We shall not attempt to calculate any of these secondary effects, and must therefore be content to compare the residue and trajectory parameters of the \hat{P} pole evaluated in the model with those extracted from the fit. We shall see that, in fact, the simple model we shall construct works quite well in this regard.

The next section is devoted to a mathematical description of the model. The numerical results are contained in Sec. III.

II. DETAILS OF THE MODEL

We shall begin with a short description of the separable-kernel method of solving the linear integral equation for the imaginary part of the $\pi\pi \rightarrow \pi\pi$ amplitude in strong coupling.² This is equivalent to doing the multiperipheral sum, and it is necessary for our discussion. The main results are presented in Eqs. (2.8), (2.17), (2.18), (2.23)–(2.32). The reader who is already familiar with this material or who does not wish to become involved in it can jump directly to these equations after reading this paragraph. The crucial point to notice is that rotation matrix functions d^{JM} and d^{jB} appear explicitly in the solutions and that these depend explicitly on the spin of the resonances involved. (One should notice that the index J_M is an s -channel spin, while j is a t -channel variable.) The solutions for the πp and $p p$ integral equations are given in the form

$$A_j(t) = A_j^0(t) + N_j(t)/D_j(t). \quad (2.1)$$

These have the same partial-wave denominator $D_j(t)$ function—that is, the leading $I_t = 0$ Regge pole in $\pi\pi$, πp , and $p p$ has the same trajectory determined by the equation $D_{\hat{\alpha}(t)}(t) = 0$. The only difference is in the partial-wave numerator $N_j(t)$ functions, and these mainly lie in the replacement of one rotation function d^J by another.

We now proceed to the solution of the integral equation itself. We write, for $\pi\pi$ elastic scattering,

$$\sigma_{tot}^{\pi\pi}(s) = \frac{1}{s} \text{Im} T_{\pi\pi}(s, 0), \quad (2.2)$$

$$\text{Im} T_{\pi\pi}(s, t) = \int_{c-i\infty}^{c+i\infty} \frac{dj}{2\pi i} (2j+1) P_j(z) A_j(t), \quad (2.3)$$

$$A_j(t) = \int_1^\infty dz Q_j(z) \text{Im} T(s, t). \quad (2.4)$$

Here, $z = z_t = \cos \theta_t$, where θ_t is the t -channel scattering angle. We have omitted the caret no-

tation \hat{A}_j , but it should be understood in all that follows, as emphasized in the Introduction.

Proceeding to partial waves through transformation Eq. (2.3) and using the diagonalization procedure of elastic t -channel unitarity equations, we arrive at the multiperipheral integral equation illustrated in Fig. 4. We introduce variables

$$\begin{aligned} 4y &= t - 2t_1 - 2t_2, & \cos\theta &= (t_1 - t_2)/2(-ty)^{1/2}, \\ 4y_0 &= t - 2m_a^2 - 2m_c^2, & \cos\theta_0 &= (m_a^2 - m_c^2)/2(-ty_0)^{1/2}, \\ 4y_f &= t - 2m_b^2 - 2m_d^2, & \cos\theta_f &= (m_b^2 - m_d^2)/2(-ty_f)^{1/2}. \end{aligned} \quad (2.5)$$

Here, y_0 and y_f are to be considered positive and

$$\begin{aligned} A_j(y_0\theta_0; y_f\theta_f; t) &= M_j(y_0\theta_0; y_f\theta_f; t) \\ &+ \frac{1}{8\pi^4} \int_0^\infty dy \int_0^\pi d\theta \frac{y \sin^2\theta}{(y + m_\pi^2 - \frac{1}{4}t)^2 + ty \cos^2\theta} M_j(y_0\theta_0; y\theta; t) A_j(y\theta; y_f\theta_f; t). \end{aligned} \quad (2.6)$$

Here, the meson resonance Born term $M_j(y_0\theta_0; y\theta; t)$ is the partial-wave projection of the meson pole term crossed to $I_t = 0$. We shall suppress the $I_t = 0$ notation. All quantities are assumed to be crossed to $I_t = 0$, and appropriate crossing matrix elements should be inserted when cross sections are calculated. We have

$$M_j(y_0\theta_0; y\theta; t) = V_{\text{off}}(y_0)V_{\text{off}}(y) \int_0^\infty dz Q_j(z) 16\pi^3 m_M^2 G^2 d_{00}^{jM}(\cos\theta_M) \delta(\bar{s} - m_M^2) \quad (2.7)$$

$$= \frac{V_{\text{off}}(y_0)V_{\text{off}}(y)}{2(y_0y)^{1/2} \sin\theta_0 \sin\theta} 16\pi^3 m_M^2 G^2 d_{00}^{jM}(\cos\theta_M) Q_j(z_M^t). \quad (2.8)$$

We have allowed for the possibility of an off-shell dependence of the $\pi\pi M$ vertex in $V_{\text{off}}(y_0)V_{\text{off}}(y)$, which is assumed factorizable for simplicity. The coupling G^2 is the isospin-0 component of the $\pi\pi M$ Born term coupling; experimentally the $I_t = 0$ coupling $G^2 \approx 0.8$ in a model with the $\pi\pi$ resonance spectrum $\{\sigma, \rho, f\}$.¹² The angle θ_M is the off-shell scattering angle for the virtual s -channel process $\pi(t_1) + \pi_a - \pi(t_2) + \pi_c$, and is given by

$$\frac{1}{2m_M^2} \lambda^{1/2}(m_a^2, t_1, m_M^2) \lambda^{1/2}(m_c^2, t_2, m_M^2) \cos\theta_M = t + \frac{1}{2}m_M^2 - \frac{1}{2}(m_a^2 + m_c^2 + t_1 + t_2) + \frac{(m_a^2 - t_1)(m_c^2 - t_2)}{2m_M^2}. \quad (2.9)$$

The variable z_M^t is *not* $\cos\theta_M$, but is rather a t -channel variable, and is given by

$$z_M^t = \frac{\cosh\beta - \cos\theta_0 \cos\theta}{\sin\theta_0 \sin\theta}, \quad (2.10)$$

where

$$\cosh\beta = (m_M^2 + y_0 + y)/2(y_0y)^{1/2}. \quad (2.11)$$

The denominator of Eq. (2.6) is the pion propagators expressed in terms of y and θ . Finally, in our simple model where $M = \rho$,

$$J_M = 1.$$

The solution of Eq. (2.6) is facilitated by the observation that y_0 and y are related to external masses and internal momentum transfers t_i . If β is large, as will be the case if $y_0y < m_M^4$, we get

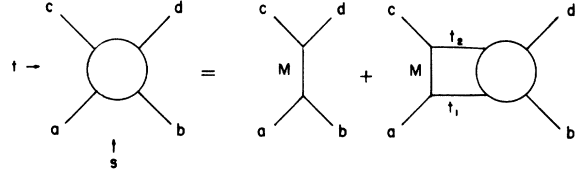


FIG. 4. Diagrammatic representation of the multiperipheral integral equation for $\pi\pi$ scattering.

analytically continued to their physical spacelike values at the end of the calculation. The equation is then, for the case of zero isospin in the t channel,²

$$\cosh\beta \approx \frac{1}{2}e^\beta \quad (2.12)$$

and, moreover, the fundamental separable approximation is valid, viz.,²

$$\cosh\beta \approx \frac{(m_M^2 + y_0)(m_M^2 + y)}{2m_M^2(y_0y)^{1/2}}. \quad (2.13)$$

Then, as z_M^t is large in this case, we use the large z_M^t limit of $Q_j(z_M^t)$. With our approximation for $\cosh\beta$, this becomes

$$Q_j(z_M^t) \approx \frac{\sqrt{\pi} \Gamma(j+1)}{\Gamma(j+\frac{3}{2})} \left[\frac{m_M^2(y_0y)^{1/2} \sin\theta_0 \sin\theta}{(m_M^2 + y_0)(m_M^2 + y)} \right]^{j+1}. \quad (2.14)$$

Actually, a more complete treatment of the problem involves an infinite sum for $Q_j(z_M^t)$, as performed in Ref. 2. We shall not enter into the

complexities caused by this, which introduce infinite determinants into the solution of the equations. We can in consequence only trust our approximation at small t .

Our approximation is called the lower-bound separable-kernel approximation to the solution.² This is because for fixed G^2 , the resulting trajectory function α is lower than the exact trajectory of the model. However, the approximation is known to be quite good at $t \approx 0$, and it has the virtue that it is valid for G^2 arbitrarily large, i.e., it is not a weak-coupling approximation.² It treats correctly the longitudinal components of momentum transfer which were incorrectly ignored in some of the papers of Ref. 4.

The separability of the equation in the variables $y_0\theta_0$ and $y\theta$ is now complete, save for the rotation function $d_{00}^{JM}(\cos\theta_M)$. This depends explicitly on all variables y_0, y, θ_0, θ in a highly complicated way. To proceed, we must imagine a separable approximation being performed as

$$d_{00}^{JM}(\cos\theta_M) = \sum_{k=1}^K V_k(y_0\theta_0; t) V_k(y\theta, t). \quad (2.15)$$

The solution given below is derived assuming d_{00}^{JM} does approximately factorize with $K=1$, though we used the explicit form of d_{00}^{JM} in our calculations. The errors introduced by this procedure are probably not substantial, and should not affect the qualitative results we shall obtain.

The solution of Eq. (2.6) is then given as

$$A_j(t) = M_j(t) + N_j(t)/D_j(t), \quad (2.16)$$

where

$$D_j(t) = 1 - \frac{1}{8\pi^4} \int_0^\infty dy \int_0^\pi d\theta \frac{y \sin^2 \theta}{(m_\pi^2 + y - \frac{1}{4}t)^2 + ty \cos^2 \theta} \times M_j(y\theta; y\theta; t). \quad (2.17)$$

The expression for $N_j(t)$ is simple. It is actually just the first iteration of Eq. (2.6) and is

$$N_j(t) = \frac{1}{8\pi^4} \int_0^\infty dy \int_0^\pi d\theta \frac{y \sin^2 \theta}{(m_\pi^2 + y - \frac{1}{4}t)^2 + ty \cos^2 \theta} \times M_j(y_0\theta_0; y\theta; t) M_j(y\theta; y_f\theta_f; t), \quad (2.18)$$

where M_j is the meson resonance Born term given by Eq. (2.8).

This completes the solution of the equation for $\pi\pi$ scattering. Given a definite prescription for V_{off} , we can now look for the leading zero of the $D_j(t)$ function by solving the equation

$$D_{\alpha(t)}(t) = 0. \quad (2.19)$$

The off-shell prescription is similar to that used

before in exclusive phenomenology,^{3,8} and is simply¹³

$$V_{\text{off}}(y) = 1 + y/m_M^2. \quad (2.20)$$

With this simple form, it is easy to show that to $O(m_\pi^2/m_M^2)$

$$D_j(0) = 1 - G^2 \Gamma^2(j)/[(j+1)\Gamma(2j)]. \quad (2.21)$$

The N_j function is then evaluated at $j = \alpha(t)$, and we obtain the final result for $\text{Im}T(s, t)$ using the inverse projection Eq. (2.3). We also use the approximation

$$(2j+1)P_j(z) \approx \frac{2\Gamma(j+\frac{3}{2})}{\sqrt{\pi}\Gamma(j+1)} \left(\frac{s}{(y_0 y_f)^{1/2} \sin\theta_0 \sin\theta_f} \right)^j \quad (2.22)$$

at $j = \alpha(t)$. One should notice at this point that the N_j function has t -channel threshold factors because the variable $\sqrt{y_0} \sin\theta_0$ is just the t -channel c.m. momentum. These are canceled out by the $P_j(z)$ function. Finally, moving the Sommerfeld-Watson integral contour to the left of the pole at $j = \alpha(t)$ yields the dimensionless $\pi\pi$ residue function $\beta_{\pi\pi}(t)$ as

$$\beta_{\pi\pi}(t) = f_{\alpha(t)} \frac{N_{\alpha(t)}(t)}{(\partial D_j/\partial j)_{j=\alpha(t)}}, \quad (2.23)$$

where

$$f_{\alpha(t)} = C_I \frac{2\Gamma(\alpha+\frac{3}{2})}{\sqrt{\pi}\Gamma(\alpha+1)} \left(\frac{m_M^2}{(y_0 y_f)^{1/2} \sin\theta_0 \sin\theta_f} \right)^{\alpha(t)}. \quad (2.24)$$

The factor C_I is the appropriate isospin crossing factor ($C_I = \frac{1}{3}$ for $\pi\pi$ scattering). Our normalization is

$$\text{Im}T_{\pi\pi}(s, t) = \beta_{\pi\pi}(t) (s/m_M^2)^{\alpha(t)}. \quad (2.25)$$

Introducing the signature factor, the full amplitude corresponding to Eq. (2.25) is

$$T_{\pi\pi}(s, t) = - \frac{\beta_{\pi\pi}(t)}{\sin(\frac{1}{2}\pi\alpha)} \left(e^{-i\pi/2} \frac{s}{m_M^2} \right)^{\alpha(t)}. \quad (2.26)$$

To find the amplitude for πp scattering is now simple. One keeps the same $D_j(t)$ function but merely substitutes a baryon resonance for a meson resonance at one end of the chain. The observant reader may worry at this point about the j -partial-wave projection in the presence of spinning external particles, since one is essentially doing a t -channel partial-wave projection of the equation, whereas the helicities of the external particles are in the s channel. This is true, but nevertheless all such problems are taken care of by the fact that as $z, z' \rightarrow \infty$ the product $d_{\lambda\mu}^j(z) e_{\lambda\mu}^j(z')$ is actually independent of λ and μ , where $e_{\lambda\mu}^j$ is

the second kind d function. Since $z = O(s/(y_0 y_f)^{1/2})$ and $z' = O(m_B^2/(y_f y)^{1/2})$, where m_B is the baryon resonance mass, this is true to the extent that our separable-kernel approximation is valid in the first place. Hence one may freely cross helicities back and forth, and the results are simply that one need not have worried about the problem in the first place. One exception to this is the case $m_B^2 = m_N^2$ for an intermediate nucleon state. Our calculation will not be performed for this case; we shall take $B = \Delta(1236)$. Hence we obtain the nonflip residue function (we suppress the helicity indices)

$$\beta_{\pi p}(t) = \frac{N_{\alpha(t)}^{\pi p}(t) f_{\alpha(t)}}{(\partial D_j / \partial j)_{j=\alpha(t)}}, \quad (2.27)$$

where the nonflip πp elastic amplitude is

$$\text{Im} T_{\pi p}(s, t) = \beta_{\pi p}(t) (s/m_M^2)^{\alpha(t)}. \quad (2.28)$$

Here,

$$N_{\alpha(t)}^{\pi p}(t) = \frac{1}{8\pi^4} \int_0^\infty dy \int_0^\pi d\theta \frac{y \sin^2 \theta}{(m_\pi^2 + y - \frac{1}{4}t)^2 + ty \cos^2 \theta} \\ \times M_\alpha(y_0 \theta_0; y \theta; t) B_\alpha(y \theta; y_f \theta_f; t), \quad (2.29)$$

where B_α is the nonflip baryon resonance Born term

$$B_\alpha(y \theta; y_f \theta_f; t) = \frac{V_{\text{off}}^B(y) V_{\text{off}}^B(y_f)}{2(y y_f)^{1/2} \sin \theta \sin \theta_f} \\ \times 16\pi^3 m_B^2 G^{B^2} d_{1/2, 1/2}^{J_B}(\theta_B) Q_\alpha(z_B^t). \quad (2.30)$$

The variables y_f and θ_f are defined in Eq. (2.5), with $m_b = m_d = m_p$. $\cos \theta_B$ is defined analogously to $\cos \theta_M$ in Eq. (2.9) in the virtual s -channel scattering $\pi(t_1) + p \rightarrow \pi(t_2) + p$. That is,

$$\lambda^{1/2}(m_B^2, m_p^2, t_1) \lambda^{1/2}(m_B^2, m_p^2, t_2) \cos \theta_B \\ = 2m_B^2 t + m_B^4 - m_B^2(2m_p^2 + t_1 + t_2) \\ + (m_p^2 - t_1)(m_p^2 - t_2). \quad (2.31)$$

We take, in accordance with our previous discussion,

$$J_B = \frac{3}{2}.$$

We shall also take $V_{\text{off}}^B = 1$. This assumes that the s -channel threshold factors in B_α are cut off rapidly as one normally does with, e.g., Benecke-Dürr or Dürr-Pilkun form factors.¹⁴

Finally, for pp elastic scattering, we simply use the fact that Regge pole residues must factorize. Hence, for double nonflip scattering, we write

$$\beta_{pp}(t) = \beta_{\pi p}^2(t) / \beta_{\pi\pi}(t). \quad (2.32)$$

The double nonflip amplitude for pp elastic scattering is then

$$\text{Im} T_{pp}(s, t) = \beta_{pp}(t) (s/m_M^2)^{\alpha(t)}. \quad (2.33)$$

We should mention that we have not calculated the spin-flip residues in this model. However, it has been shown that the ABFST model⁵ is in fact consistent with approximate s -channel helicity conservation for the leading $I_t = 0$ pole when a spectrum of πN resonances is included.¹⁵ The mechanism for the suppression of the flip/nonflip amplitude ratio is that cancellations among the πN resonance contributions occur in the flip amplitude but not in the nonflip amplitude. Since a more complete treatment of residues in our model would of course include the πN resonance spectrum we simply invoke the results of Ref. 15 to ignore the \hat{P} spin-flip residues. This is consistent with two-body data.¹⁰

This ends our discussion of the model. We emphasize once more that the essence of our model is that the resonance spins are responsible for the difference between the πp and pp differential cross section slopes. This is due to the fact that $J_B > J_M$. Here $J_M = 1$ and $J_B = \frac{3}{2}$, so that

$$d_{00}^{J_M}(\cos \theta_M) = \cos \theta_M, \quad (2.34) \\ d_{1/2, 1/2}^{J_B}(\cos \theta_B) = \frac{1}{2} \cos \frac{1}{2} \theta_B (3 \cos \theta_B - 1).$$

III. RESULTS

In this section we present the results of our calculations. These were performed by computer evaluation of the two-dimensional integrals for $N_\alpha(t)$ and $D_\alpha(t)$ described in the last section. We shall present the results with the correct spin structure of the resonances and we shall show that this is indeed the relevant effect by presenting graphs obtained by setting the $d_{00}^{J_M}$ and $d_{1/2, 1/2}^{J_B}$ functions equal to 1. The graph of the trajectory $\alpha(t)$ obtained by solving the equation $D_\alpha(t) = 0$ numerically is shown in Fig. 5. The solid curve is the result of the model with $J_M = 1$, $J_B = \frac{3}{2}$. The dashed curve is the result for spinless clusters.

We have set the intercept of the trajectory equal to 0.85. This reflects our philosophy that the trajectory function calculated in this model is really the bare Pomeron trajectory $\hat{\alpha}(t)$ (see Introduction).⁷ The phenomenology of meson-nucleon two-body reactions performed in Ref. 10 indicates

$$\hat{\alpha}(t) = 0.85 + 0.3t. \quad (3.1)$$

Our trajectory is somewhat curved, but over the range $-0.3 \text{ GeV}^2 < t \leq 0$, it is reasonably well represented by a linear trajectory with slope $\frac{1}{2}$. That

is,

$$\alpha(t)|_{\text{model}} \approx 0.85 + 0.5t . \quad (3.2)$$

The agreement of the model with the t dependence of the actual bare Pomeron trajectory determined from the data is impressive, considering the simplicity of the model. In particular this implies that the energy dependence of the slope parameter is given in a very reasonable way in the model. Here, the spin structure is not as important as the correct treatment of kinematics, as Jadach and Turnau have argued.⁴

The intercept 0.85 is somewhat higher than that obtained with the physical value of the $I_t=0$ coupling $G^2 \approx 0.8$, but the value of G^2 we need is within a factor of 2 of this. Better agreement would result if higher-order clusters were included, and we shall see that higher-order clusters are also probably necessary to get the multiplicity distribution correct. We shall not go beyond $t = -0.3 \text{ GeV}^2$ in what follows, since our approximations of the last section indicate that our results can be reliable only to $O(-t/m_\rho^2)$, which we should require to be less than 1.

Next we consider the residue functions for $\pi\pi$ elastic scattering, nonflip πp elastic scattering, and double nonflip pp elastic scattering. The residue functions, divided by $\sin(\frac{1}{2}\pi\alpha)$, are plotted in Fig. 6. We have used the physical values $m_M^2 = m_\rho^2$ and $m_B^2 = m_\Delta^2$. Again, we show curves with and without spin. We see that, in the range $-0.3 < t < 0$, the $\pi\pi$ residue function is roughly flat, while the πp residue function decreases in $|t|$. By factorization, the pp residue function decreases faster

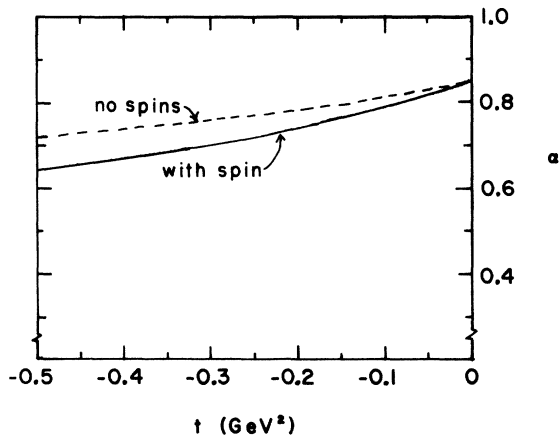


FIG. 5. Bare Pomeron trajectory $\hat{\alpha}(t)$ versus t , as calculated by the model (solid curve). The dashed curve shows the trajectory resulting from a model with spinless clusters.

yet. This confirms our initial belief that the difference in the ρ and Δ resonance spins would lead to higher peripherality when pion external legs are replaced by nucleons. These results should be compared with the dashed curve obtained by neglecting the spins of the resonances. When this is done, there is no peripherality for any of the residue functions, and they are in fact indistinguishable. This graphically illustrates the crucial importance of the spin of the clusters.

To compare our results with experimental data, we first approximate the πp residue function with an exponential. A glance at Fig. 6 shows that $\beta_{\pi p}$ is not really exponential—there was no expectation or constraint that it would be exponential. Nevertheless, over the range $-0.3 < t < 0$, $\beta_{\pi p}/\sin(\frac{1}{2}\pi\alpha)$ is reasonably well represented by

$$R_{\pi p}(t) \equiv \frac{\beta_{\pi p}(t)}{\beta_{\pi p}(0)} \frac{\sin(\frac{1}{2}\pi\alpha(0))}{\sin(\frac{1}{2}\pi\alpha(t))} \approx e^{1.2t} . \quad (3.3)$$

Thus, our bare Pomeron pole amplitude for nonflip πp scattering, for $P_{\text{lab}} < 30 \text{ GeV}/c$ and $-0.3 < t < 0$, is roughly

$$T_{\pi p}^{\hat{P}}(s, t)|_{\text{model}} = - \frac{\beta_{\pi p}(0)}{\sin(\frac{1}{2}\pi\alpha(0))} \times e^{1.2t} \left(e^{-i\pi/2} \frac{s}{m_\rho^2} \right)^{0.85+0.5t} \quad (3.4)$$

Notice that m_ρ^2 sets the scale for s in the model.

In order to compare this with the data, we again refer to the global meson-nucleon fit in Ref. 10.

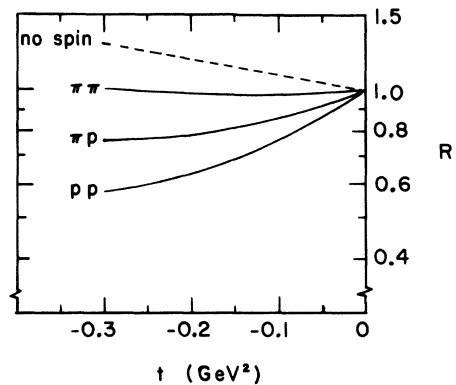


FIG. 6. Residues predicted by the model, divided by $\sin(\frac{1}{2}\pi\alpha(t))$, normalized to 1 at $t=0$. The solid curves show $R_{\pi\pi}$, $R_{\pi p}$, and R_{pp} , assuming correct spins for the appropriate resonances. The dashed curve shows the result for spinless clusters; $R_{\pi\pi}$, $R_{\pi p}$, and R_{pp} are indistinguishable in this case. See Eqs. (3.4), (3.7).

In that fit, it was found that

$$T_{\pi p}^{\hat{P}}(s, t)|_{\text{fit}} = -C e^{Bt} \left(e^{-i\pi/2} \frac{s}{s_0} \right)^{0.85+0.3t}, \quad (3.5)$$

where

$$B \approx 1.6 \text{ GeV}^{-2},$$

$$s_0 = 1 \text{ GeV}^2.$$

If our residue function is reasonably accurate, we would expect that

$$b_{\pi p} \approx 1.2 + 0.5 \ln(s_0/m_p^2) \stackrel{?}{=} B. \quad (3.6)$$

The left-hand side of this comparison is 1.4 GeV^{-2} . Again, considering the simplicity of the model, the agreement is remarkable.

We unfortunately cannot make a reliable comparison of our results for the bare Pomeron component of pp elastic scattering because no such fits have yet been performed for nucleon-nucleon scattering. It is wrong, of course, to compare our results directly with $(d/dt) (\ln d\sigma/dt)$, because at intermediate energies, absorptive cuts and secondary trajectories play a significant role. We shall try to make a rough estimate by comparing the *difference* between πp and pp slopes. Our model predicts that, for the bare Pomeron component of double nonflip pp scattering,

$$T_{pp}^{\hat{P}}(s, t) \approx - \frac{\beta_{\pi p}^2(0)}{\beta_{\pi\pi}(0) \sin(\frac{1}{2}\pi\alpha(0))} \times e^{2.4t} \left(e^{-i\pi/2} \frac{s}{m_p^2} \right)^{0.85+0.5t} \quad (3.7)$$

In analogy to Eq. (3.6), the constant part of the diffractive slope in the model is

$$b_{pp} \approx 2.4 + 0.5 \ln(s_0/m_p^2) = 2.6 \text{ GeV}^{-2}. \quad (3.8)$$

Hence, the constant part of the \hat{P} contribution to the slope of $d\sigma/dt|_{pp}$ is $2b_{pp} = 5.2 \text{ GeV}^{-2}$. The difference in the \hat{P} component of the pp and πp diffractive slopes near $t=0$ is then

$$\begin{aligned} \frac{d}{dt} \left(\ln \frac{d\sigma}{dt} \right)_{pp} - \frac{d}{dt} \left(\ln \frac{d\sigma}{dt} \right)_{\pi p} &= 2b_{pp} - 2b_{\pi p} \\ &= 2.4 \text{ GeV}^{-2}. \end{aligned} \quad (3.9)$$

Experimentally, the difference is of this order.¹⁶ The interested reader may consult Ref. 1 for a separate experimental comparison of pp slopes.

As for the $\pi\pi$ residue, naturally little is known about it experimentally. Our calculation predicts that the peripherality of the \hat{P} component of $\pi\pi$ scattering is due almost entirely to the factor

$$(s/m_p^2)^{\hat{\alpha}(t)}.$$

$d\sigma/dt$ for $\pi\pi$ scattering should be less peripheral than for πp scattering. By analogy with our discussion of pp scattering, we predict

$$2b_{\pi p} - 2b_{\pi\pi} \approx 2.4 \text{ GeV}^{-2}.$$

This number could be compared with experimental data for $d\sigma/dt|_{\pi\pi}$. Indications from experiment are that $b_{\pi\pi}$ is indeed less than $b_{\pi p}$, and that the difference is on the order of that given by our model.¹⁷

We close our discussion of slopes with an account of Kp scattering. This is easy to accommodate. We merely insist that the incident K meson fragments into a $K^*(890)$ at the end of the chain. Since $J_M = 1$ for this case also (and since mass effects have been shown to be negligible), we obtain exactly the same result for the \hat{P} component in Kp as in πp scattering, i.e.,

$$b_{Kp} \approx 1.4 \text{ GeV}^{-2}.$$

Since the universal number $B = 1.6 \text{ GeV}^{-2}$ fits the \hat{P} component of the Kp data as well as the πp data, we conclude that the model works here as well.

Finally, we check the multiplicity distribution produced by the model. Since our model is multiperipheral in clusters, the average multiplicity of produced particles is arbitrary until the number of particles in the clusters is specified. The calculation of the trajectory and residue parameters, on the other hand, depends only on the over-all properties of a cluster, e.g., its spin—but not on the number of its constituent particles. We have,³ neglecting secondary cuts and poles,

$$\frac{\langle n \rangle}{\ln s} = \frac{n_c}{(\partial D_j / \partial j)_{j=\hat{\alpha}(0)}}, \quad (3.10)$$

where $\langle n \rangle$ is the average number of produced particles, and n_c is the average number of particles per cluster. Experimentally,¹⁸ for $P_{\text{lab}} < 30 \text{ GeV}/c$, where our model is supposed to be applicable,

$$\frac{\langle n \rangle}{\ln s} \approx 1.5 - 2.0, \quad (3.11)$$

where the exact value is ambiguous owing to the presence of secondary terms down by fractional powers of s . It is important to realize that since we are taking the position that important threshold effects are present above $30 \text{ GeV}/c$ (e.g., $K\bar{K}$, $B\bar{B}$ production and inelastic diffraction), we must *not* utilize Fermilab-ISR multiplicity data, which produce $\langle n \rangle / \ln s \approx 3$. Any attempt to incorporate the renormalization effects to determine $d\sigma/dt$ slopes at Fermilab-ISR energies would, of course, require consistency with multiplicity data at these energies.

Our intermediate-energy model produces

$$(\partial D_j / \partial j)_{j=\alpha(0)} = 2.4, \quad (3.12)$$

so that $n_c = 3 - 5$. We would naturally argue that the secondary terms in $\langle n \rangle / \ln s$ were such that n_c was closer to 3. In any case, this indicates the presence of higher-order clusters than the simple resonances we have employed in this calculation. An alternative may be to modify the exchange mechanisms of the model to produce a smaller value of $\partial D_j / \partial j$, consistent with smaller clusters.

We close with a remark regarding momentum transfer distributions. Multi-Regge models which neglect longitudinal components of momentum transfer arrive at a relation⁴ between α' , $\langle n \rangle$, and the average transverse momentum of produced particles $\langle p_{\perp}^2 \rangle$. This relation is violated by the data; it is also theoretically wrong. The correct relation is given by

$$(\partial D_j / \partial j)^{-1} = \alpha' (-\partial D_j / \partial t)^{-1} = \langle n \rangle / (n_c \ln s) \quad (3.13)$$

evaluated at $j = \alpha(0)$ and $t = 0$. There is no direct experimental constraint on $\partial D_j / \partial t$. It is instructive to note that momentum transfer and transverse momentum distributions are wildly differ-

ent experimentally.¹⁹ Our model does in fact reproduce these distributions correctly qualitatively when evaluated by computer methods.⁸

IV. SUMMARY

We have shown that a multiperipheral cluster model is capable of yielding reasonable results for the \hat{P} components of the slope in t of the differential cross sections for πp , Kp , and pp elastic scattering below 30 GeV/c. This is consistent with a reasonable trajectory for \hat{P} and a sensible average multiplicity of produced particles. The crucial aspect of our model is the cluster spin effect and the realization that, on the average, the baryon resonance spin is half a unit greater than the meson resonance spin. We envisage that a more complete calculation involving a more complicated resonance spectrum would yield similar qualitative results, and that one could even turn the problem around to inquire about the detailed nature of clusters in production processes by utilizing the t slope of $d\sigma/dt$ as a constraint.

*Work performed under the auspices of the U. S. Atomic Energy Commission.

†Present address: Department of Physics, University of Oregon, Eugene, Oregon 97403.

‡Work supported in part by the Research Corporation.

¹A summary of this work is contained in J. W. Dash and S. T. Jones, Phys. Lett. **55B**, 212 (1975).

²For a discussion of multiperipheral models and the strong coupling separable kernel techniques used here see J. W. Dash, Nuovo Cimento **9A**, 265 (1972); M. L. Goldberger, in *Developments in High Energy Physics*, proceedings of the International School of Physics "Enrico Fermi," Course LIV, 1971, edited by R. Gatto (Academic, New York, 1972), p. 1. Regge slopes are discussed in J. W. Dash, Nuovo Cimento **8A**, 787 (1972).

³J. W. Dash, G. Parry, and M. Grisaru, Nucl. Phys. **B53**, 91 (1973); J. W. Dash, Phys. Rev. D **8**, 2987 (1973).

⁴For previous work on this subject see R. C. Hwa, Phys. Rev. D **8**, 1331 (1973); C. Hamer and R. F. Peierls, *ibid.* **8**, 1358 (1973); S. Jadach and J. Turnau, Phys. Lett. **50B**, 369 (1974); F. Henyey, *ibid.* **B45**, 469 (1973); Nucl. Phys. **B78**, 435 (1974); F. Henyey, R. Hong Tuon, and G. Kane, *ibid.* **B70**, 445 (1974); M. Teper, Westfield College report, 1974 (unpublished); T. Ueda, Osaka Univ. report, 1974 (unpublished); H. W. Wyld, Phys. Rev. D **3**, 3090 (1971).

⁵D. Amati, A. Stanghellini, and S. Fubini, Nuovo Cimento **26**, 896 (1962); D. Avalos and B. Webber, Phys. Rev. D **4**, 3313 (1971); C. Chan and B. Webber, *ibid.* **5**, 933 (1972). Some disagreement with the latter two papers can be traced to an incorrect excessive high-spin component (g) in the former and the use of on-

shell kinematics for the virtual angle θ_M in the latter.

⁶E. M. Gordon and R. Hwa, Nucl. Phys. **B68**, 433 (1974). See also Z. Ajduk, Nuovo Cimento **16A**, 111 (1973).

These authors work within the framework of certain inelastic diffraction models.

⁷J. W. Dash, Phys. Lett. **49B**, 81 (1974).

⁸J. W. Dash, J. Huskins, and S. T. Jones, Phys. Rev. D **9**, 1404 (1974); J. W. Dash and S. T. Jones, *ibid.* **9**, 2539 (1974).

⁹J. W. Dash, Phys. Rev. D **9**, 200 (1974).

¹⁰N. F. Bali and J. W. Dash, Phys. Lett. **51B**, 99 (1974); Phys. Rev. D **10**, 2102 (1974).

¹¹J. W. Dash and J. Koplik, Columbia Univ. Report No. C0-2271-45 (rev.) (unpublished).

¹²(a) G. F. Chew, T. Rogers, and D. Snider, Phys. Rev. D **2**, 765 (1970); (b) R. Blankenbecler, Phys. Rev. Lett. **31**, 964 (1973).

¹³This form for V_{off} is that used in Ref. 3 to generate the bare Pomeron. It should be noted that it is taken for simplicity as independent of the s -channel partial-wave value J_M . Indeed, it is implicitly assumed that the threshold behavior in J_M is damped out rapidly, leaving Eq. (2.20) as the effective behavior for the relevant ranges of momentum transfer. The observant reader may worry about convergence problems. The lower-bound approximation itself provides an effective cutoff to make all integrals converge.

¹⁴H. P. Dürr and H. Pilkuhn, Nuovo Cimento **40**, 899 (1965); J. Benecke and H. P. Dürr, *ibid.* **56**, 269 (1968).

¹⁵S. Islam, Nucl. Phys. **B41**, 226 (1972).

¹⁶See, e.g., Yu. M. Antipov *et al.*, Nucl. Phys. **B57**, 333 (1973).

¹⁷W. J. Robertson, W. D. Walker, and J. L. Davis, Phys. Rev. D 7, 2554 (1973).

¹⁸E. Berger, B. Oh, and G. Smith, Phys. Rev. Lett. 29, 675 (1972); O. Czyżewski and K. Rybicki, Nucl. Phys. B47, 633 (1972).

¹⁹Cf. M. Bardadin-Otwinowska *et al.*, Phys. Rev. D 4,

2711 (1971). See also Ian Halliday, rapporteur's talk in *Proceedings of the XVII International Conference on High Energy Physics, London, 1974*, edited by J. R. Smith (Rutherford Laboratory, Chilton, Didcot, Berkshire, England, 1974), p. I-229.